Neurochemical Research (2025) 50:171
https://doi.org/10.1007/s11064-025-04419-6

RESEARCH

Study on the Mechanism of Dihydromyricetin in Alleviating Depressive-Like Behavior in Rats Based on Network Pharmacology

Xue Li[1] · Miaoqi Chen[1] · Decheng Wei[1] · Pengsheng Wei[1] · Yanzong Jiang[1] · Jiaqi Chen[1] · Xiaomeng duan[2] · Zitong Wang[3] · Yuchuan Zhang[1] · Dafeng Bai[4] · Hui Jia[2,5] · Ge Jin[2,5]

Received: 27 December 2024 / Revised: 1 May 2025 / Accepted: 5 May 2025 / Published online: 26 May 2025

Abstract

Depression is a chronic and recurrent neuropsychiatric disorder with complex pathophysiology. Dihydromyricetin (DMY), a bioactive flavonoid compound isolated from Ampelopsis grossedentata (commonly known as rattan tea), has demonstrated multiple pharmacological properties including anti-inflammatory, antioxidant, antitumor, and antimicrobial activities. In the present study, a well-established rodent model of depression was generated through chronic unpredictable mild stress (CUMS) paradigm combined with social isolation. Following eight weeks of DMY intervention, comprehensive behavioral assessments were conducted to validate both the successful establishment of the depression model and the therapeutic efficacy of DMY treatment. We employed network pharmacology approaches to systematically predict potential antidepressant targets of DMY. Further mechanistic investigations were performed to elucidate the underlying molecular pathways, providing novel perspectives for developing innovative antidepressant therapeutics.Integrating network pharmacology prediction with molecular biology validation, our findings revealed that DMY exerts significant antidepressant-like effects through suppression of the advanced glycosylation end products (AGEs)-RAGE signaling pathway, activation of the nuclear factor E2-related factor 2 (NRF2)-mediated antioxidant defense system, and upregulation of synaptic plasticity-related proteins including postsynaptic density protein 95 (PSD95) and synaptophysin (SYP). These results suggest that DMY may represent a promising natural therapeutic candidate for depression treatment.

Keywords Depression · Dihydromyricetin · Network pharmacology · Anti-inflammatory · Oxidative stress

Introduction

Depression is a persistent and recurring mental health condition characterized by its prolonged duration. It is often resistant to treatment and is characterized by high rates of relapse, medication withdrawal symptoms, morbidity, and an

Xue Li, Miaoqi Chen and Decheng Wei are the co-first authors.

✉ Dafeng Bai
dafengbai@163.com

✉ Hui Jia
huijia412413@symc.edu.cn

✉ Ge Jin
jinge1026@163.com

[1] Basic Medical School, Shenyang Medical College, 146 Huanghe North Street, Yuhong District, Shenyang 110034, Liaoning, China

[2] School of Traditional Chinese Medicine, Shenyang Medical College, 146 Huanghe North Street, Yuhong District, Shenyang 110034, Liaoning, China

[3] School of Pharmacy, Shenyang Medical College, 146 Huanghe North Street, Yuhong District, Shenyang 110034, Liaoning, China

[4] The Eleventh People's Hospital of Shenyang, No. 31 Haitang Street, Shenyang, China

[5] Key Laboratory of Behavioral and Cognitive Neuroscience of Liaoning Province, Shenyang Medical College, 146 Huanghe North Street, Yuhong District, Shenyang 110034, Liaoning, China

elevated risk of suicide [1]. Based on the most recent information from the World Health Organization (WHO), it is estimated that more than 350 million individuals around the globe are experiencing depression [2–4]. In more than three-quarters of depression cases, symptoms of this condition will manifest repeatedly and persistently throughout the lifetime of an individual [5]. Depression not only leads to significant mental distress but also disrupts sleep, appetite, metabolic activity, and fundamental biological processes, such as autonomic function and neuroendocrine regulation [6]. Maes and Vandoolaeghe [7] were the pioneers in proposing the inflammatory hypothesis, grounded in their observation of a systemic inflammatory state present in patients suffering from major depression. They proposed that there may be a close association between the onset of depression and the systemic inflammatory response. The core hypothesis of this theory posits that under conditions of inflammation, inflammatory cytokines, like tumor necrosis factor-α (TNF-α) and interleukin-1β (IL-1β) increase while anti-inflammatory factors decrease. This results in an overstimulation of the immune system, which subsequently disrupts the balance between neuroendocrine and immune functions. It leads to sustained inflammation, ultimately contributing to the development of depression. Clinical research has indicated that individuals undergoing treatment with interferon (IFN) and interleukin-2 (IL-2) frequently exhibit symptoms of depression frequently [8]. These symptoms typically resolve after medication withdrawal. Animal experiments have also manifested that inflammatory triggers can induce depression-like behaviors in animals. These are reversible after the administration of antidepressant drugs. Conversely, inhibiting cytokine activity or eliminating its receptors has demonstrated antidepressant effects [9]. Recently, there has been an increased exploration and refinement of the inflammatory cytokine hypothesis in relation to depression. Prolonged, unpredictable mild stimulation has been proposed to have an adverse effect on the neuroendocrine system by excessively stimulating both the peripheral and central immune responses. This results in the release of a significant amount of inflammatory factors, a decrease in monoamine neurotransmitters, and excessive and persistent activation of the HPA axis-induced apoptosis. In the end, this affects the progression of depression.

The AGEs—RAGE signaling pathway,which is an inflammatory pathway [10], has been identified as a critical contributor to the onset of diabetic complications and a range of chronic illnesses, including cardiovascular diseases, neurodegenerative conditions (e.g., Alzheimer's disease (AD), Parkinson's disease (PD)), cancer, and related issues [11]. AGEs are generated during the later phases of the Maillard reaction, in which proteins, amino acids, lipids, or nucleic acids react with free amino groups and reducing sugars—such as glucose, fructose, and pentose—resulting when forming stable compounds through carbonyl reactions [12]. In response to elevated glucose levels, inflammation, and oxidative stress, AGEs can trigger numerous signaling pathways through their interaction with the receptor for RAGE located on the cell surface. This process involves the phosphorylation of phosphatidylinositol-3-kinase (PI3K) and protein kinase B (AKT). This subsequently results in an atypical activation of nuclear transcription factor (NF)-κB, as the primary regulatory transcription factor in inflammation. NF-κB takes charge of regulating gene expression of inflammatory cytokines like TNF-α and IL-1β. It thereby initiates a response characterized by inflammation. Repetitive exposure to oxidative stress may increase the formation of AGEs [13], activate RAGE, and subsequently increase nicotinamide adenine dinucleotide phosphate (NADPH) oxidase activity, resulting in the overproduction of reactive oxygen species (ROS). We hypothesized that the AGEs-RAGE pathway activates ROS production via NADPH oxidase, leading to oxidative stress and subsequent neuroinflammation. The NRF2 pathway is considered the major mechanism for inducing endogenous antioxidant stress in the body. The fundamental pathophysiological mechanism of depression involves the abnormal regulation of neuroplasticity [14]. This diminishes synaptic plasticity, representing the predominant pathological alteration in individuals affected by depression [15–17].

Given the involvement of AGEs-RAGE in neuroinflammation and oxidative stress, targeting this pathway with anti-inflammatory compounds like DMY may offer therapeutic potential for depression. DMY, a naturally occurring flavonoid obtained from ampelopsis grossedentata, exhibits various pharmacological effects. These properties encompass anti-inflammatory [18], anti-tumor [19], anti-oxidant [20], anti-infective, and neuroprotective effects, particularly within the realm of neurodegenerative diseases [21, 22]. Recent studies indicate that DMY possesses neuroprotective properties and shows potential for alleviating a range of neurological disorders, such as alcohol addiction, AD, PD. It demonstrates notable therapeutic efficacy for treating PD, ischemic stroke and alcohol addiction [23]. DMY improves PD by acting on gamma-aminobutyric acid type A receptor ($GABA_a$) and Free Fatty Acid Receptor 3 (FA3R) pathways [24]. DMY, by acting as a positive allosteric modulator of $GABA_a$ receptors, restoring gephyrin expression, and remodeling the density, size, and morphology of hippocampal astrocytes. This leads to improvements in cognitive deficits, anxiety, and astrocytic irregularities caused by social isolation [25].

CUMS is a well-validated and non-invasive method for establishing a depression model [26]. CUMS combined with social isolation represents a novel depression model [27], which has been verified through multiple experiments [28–30]. Based on this, we established an animal model

of depression using CUMS combined with social isolation to investigate whether DMY improves the condition of depressed rats by targeting the AGEs-RAGE signaling pathway (Fig. 1).

Results

Effect of DMY on Anxiety-Like Behavior in the Open Field Test (OFT)

In comparison to the control group, the depression model group exhibited significantly reduced time spent ($p < 0.01$) and distance traveled ($p < 0.001$) in the central zone during the OFT. Compared with the model group, the 40 mg/kg DMY group showed a significant increase in both the activity time and the moving distance in the central area ($p < 0.05$). Moreover, the 80 mg/kg DMY group and the fluoxetine treatment group demonstrated further improvements in these parameters ($p < 0.01$) (Fig. 2C–E).

Effect of DMY on Cognitive Function in Depressive Model Rats of Y-Maze Test

In the Y-maze, no notable differences could be found in the spontaneous alternation rate among the five groups (Fig. 2F). Nevertheless, the depression model group exhibited a substantial decrease in the number of arm entries compared to the control group ($p < 0.001$). Conversely, both the DMY (40 mg/kg and 80 mg/kg) and fluoxetine treatment groups showed a significant increase in the number of arm entries when compared to the depression model group ($p < 0.01$). These findings indicate that DMY may enhance exploratory behavior in depression model (Fig. 2G).

Effect of DMY on Anxiety and Depression-Like Behaviors in Depressive Model Rats of Multi-Function Closed Maze (MCM)

Compared with the control group, the model group showed significantly decreased activity frequency and total distance in the MCM ($p < 0.001$, $p < 0.01$). The 40 mg/kg DMY, 80 mg/kg DMY, and fluoxetine exhibited increased activity frequency ($p < 0.05$, $p < 0.01$, $p < 0.05$) and total distance traveled ($p < 0.05$) when compared to the model group (Fig. 2H, I). The trajectory and hot zone diagrams further illustrate these findings (Fig. 2J, K).

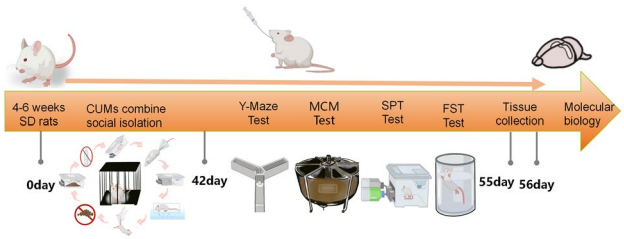

Fig. 1 Experimental flowchart

Effect of DMY on Depression-Like Behaviors in Sucrose Preference Test (SPT)

The SPT was developed in accordance with rodents' natural inclination towards sweet substances, making it the most reliable approach for evaluating anhedonia in rat models. Pure water consumption in the SPT did not reveal any notable differences between the five groups of rats (Fig. 2L).However, in contrast to the control group, the sucrose preference ratio was significantly reduced in the model group ($p < 0.001$). In comparison with the model group, the fluoxetine treatment, 40 mg/kg DMY, and 80 mg/kg DMY group, exhibited a significant increase in the sucrose preference ratio ($p < 0.01$) (Fig. 2M).

Effect of DMY on Depression-Like Behaviors in Novelty-Suppressed Feeding Test (NSFT)

In the NSFT, the depression model group exhibited a significantly prolonged latency to the first feeding compared to the control group ($p < 0.001$) (Fig. 2N). The frequency of standing times was greatly decreased ($p < 0.01$) (Fig. 2O). Compared with the depression model group, notable reductions in the latency of the first feeding were observed in the fluoxetine treatment, 40 mg/kg DMY, and 80 mg/kg DMY group ($p < 0.05$), alongside a significant increase in the number of standing times ($p < 0.05$).

Effect of DMY on Depression-Like Behaviors in Forced Swimming Test (FST)

In the FST, compared with the control group, the immobility time of the rats in the depression model group was significantly prolonged ($p < 0.001$). The treatment groups (the fluoxetine treatment group, the 40 mg/kg DMY group and the 80 mg/kg DMY group) all showed a significant reduction in immobility time ($p < 0.05$, $p < 0.05$, $p < 0.01$), among which the improvement effect of the high-dose DMY group was particularly prominent (Fig. 2P). The above results indicate that DMY reduces the manifestation of behavioral despair and effectively alleviates the depression-like behaviors of rats.

Results of Network Pharmacology Experiments

Target Screening of DMY and Depression

After integrating the corresponding targets of DMY into the Traditional Chinese Medicine Systems Pharmacology

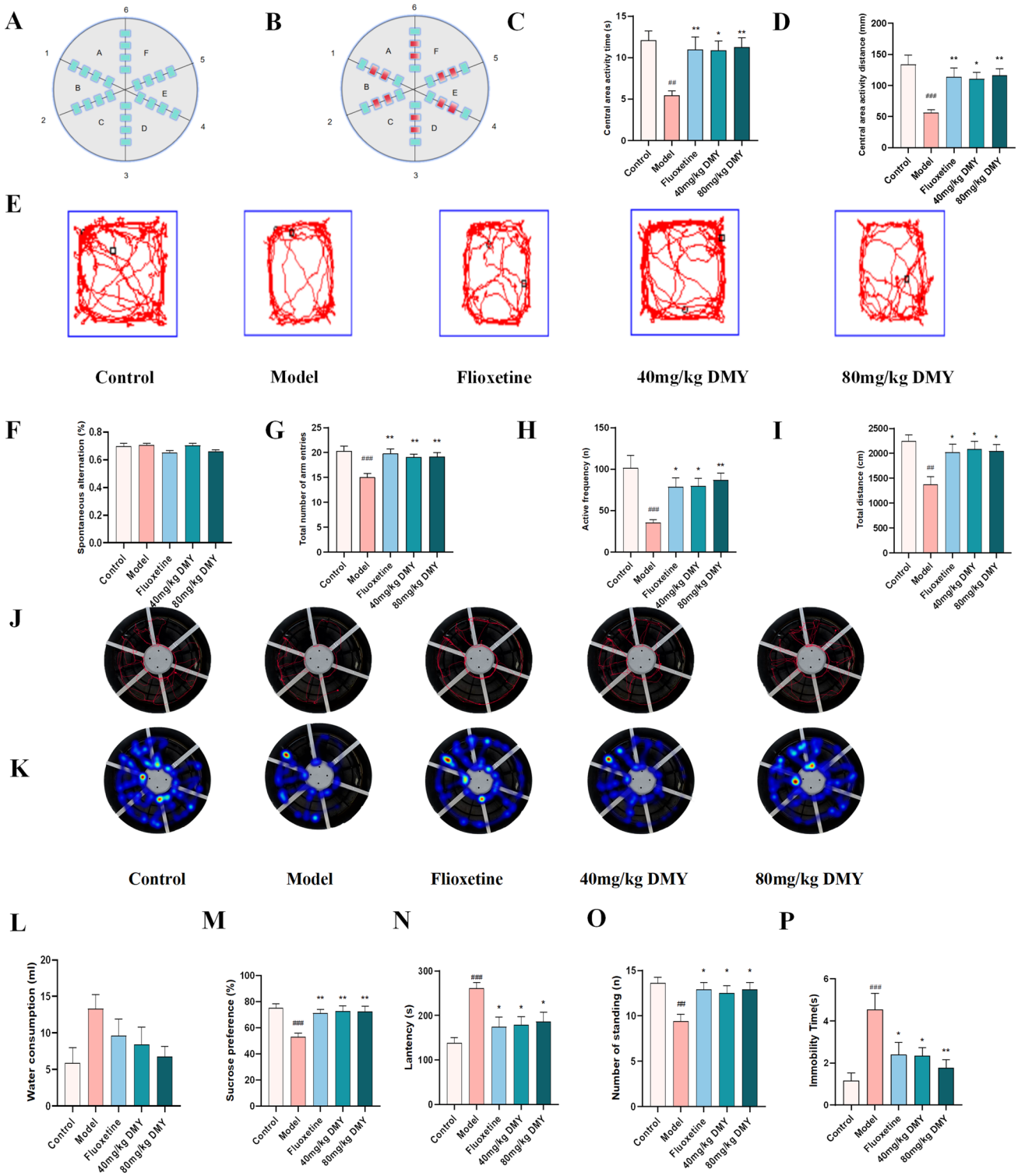

Fig. 2 **A**: Maze design for the first day of adaptation in the MCM; **B**: Experimental design for the second-day test phase in the MCM. **C**: Activity time in the central area in the OFT; **D**: Movement distance in the central area in the OFT; **E**: all groups on behalf of the trajectory in the OFT. **F**: Spontaneous alternating response rate in the Y-maze; **G**: Number of maze entries in the Y-maze. **H**: Active frequency in the MCM; **I**: Moving distance in the MCM; **J**: Trajectory diagram in the MCM; **K**: Hot zone map in the MCM. **L**: The pure water consumption in the SPT; **M**: The sugar water preference ratio in the SPT. **N**: Feeding latency in the NSFT; **O**: The number of standing times of rats in the NSFT. **P**: Immobility time in FST. MCM Experimental apparatus walls blue door to open says in an open position to allow through; the red door is closed, impassable. All data are expressed as Mean ± SEM (n = 10). ##$p < 0.01$ and ###$p < 0.001$ vs.control, *$p < 0.05$ and **$p < 0.01$ vs. model

Database and Analysis Platform (TCMSP, https://tcmsp-e.com/tcmsp.php [31]), SwissTargetPrediction (http://www.swisstargetprediction.ch/ [32]), and PharmMapper (https://www.lilab-ecust.cn/pharmmapper/index.html [33]) databases, a total of 86 unique protein targets were identified after eliminating duplicates. By combining the search results of five disease-related databases-GeneCards (https://www.genecards.org/ [34]), Online Mendelian Inheritance in Man (OMIM, https://omim.org/ [35]), The Pharmacogenomics Knowledgebase (PharmGKB, https://www.pharmgkb.org/ [36]), Therapeutic Target Database (TTD, http://db.idrblab.net/ttd/ [37]), and DrugBank (https://go.drugbank.com/ [38]) and removing duplicates, 11,757 protein targets associated with depression were identified (Fig. 3A). A total of 79 protein targets were identified as common targets of DMY and depression. These were considered potential targets for the management of depression by DMY.A network diagram of the intersecting targets of DMY and depression is depicted in (Fig. 3B).

Construction of Protein – Protein Interaction (PPI) Network

The 79 potential targets of DMY for depression were imported into the STRING platform (https://cn.string-db.org [39]) to construct a PPI network (Fig. 3C). The PPI network comprised 79 nodes and 1,080 edges, resulting in an average degree of 27.34. The STRING platform for PPI network information was visualized using the Cytoscape (3.8.0) software (Fig. 3D). These targets included DMY, which is a key target for treating depression. According to the network topology analysis of the degree values (Fig. 3E), the targets with higher degree values included epidermal growth factor receptor (EGFR), Cysteine-aspartic Protease 3 (Caspase-3), B-cell lymphoma 2 (BCL2), Hypoxia-Inducible Factor 1 Subunit Alpha (HIF1A), and amyloid precursor protein (APP).

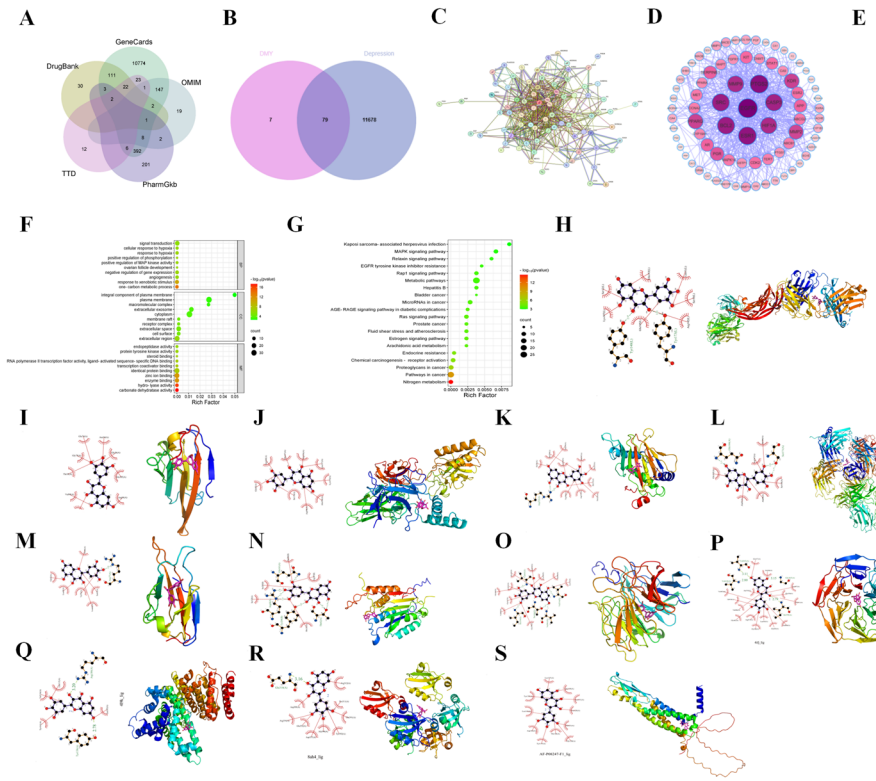

name	Degree
EGFR	88
PTGS2	82
ESR1	80
SRC	76
BCL2	76
Caspase-3	74
MMP9	70
HIF1A	70
KDR	60
PPARG	60
MMP2	58
PGR	52
SERPINE1	48
APP	46

Name	Compound	Name	Compound
VEGFA	-6.2	IL- 1β	-7.0
AGEs	-6.6	RAGE	-7.2
NF-κB	-6.7	Caspase-3	-7.3
HIF1A	-6.9	NRF2	-8.8

Fig. 3 **A**: Depression targets; **B**: DMY-depression intersection targets Venn diagram; **C**: PPI network diagram of STRING platform; **D**: Target PPI network diagram; **E**: Related targets corresponding values; **F**: GO enrichment analysis; **G**: KEGG signaling pathway enrichment analysis. Docking diagram of DMY and protein molecules: **H**: VEGFA (PDB ID:1BJ1) -DMY; **I**: AGEs (PDB ID:2MOV) -DMY; **J**: NF-κB (PDB ID:1A3Q) -DMY; **K**: HIF1A (PDB ID:3HQU) -DMY; **L**: IL-1β (PDB ID:5BVJ) -DMY; **M**: RAGE (PDB ID:2E5E) -DMY; **N**: Caspase-3 (PDB ID:1NME)-DMY; **O**: NRF2 (PDB ID:2FLU) -DMY; **P**: Keap1 (PDB ID:4IFJ)-DMY; **Q**: HO-1 (PDB ID:4L9K)-DMY; **R**: PSD95 (PDB ID: 8ah4)-DMY; **S**: SYP (AlphaFold ID: AF-P08247-F1)-DMY. **T**: Molecular docking binding energy rating (kJ/mol)

Gene Ontology (GO) and Kyoto Encyclopedia of Genes and Genomes (KEGG) Pathway Enrichment

The 79 potential targets of DMY for depression were subsequently incorporated into the DAVID database for enrichment analysis. The functional enrichment analysis (Fig. 3F) yielded 420 GO terms, comprising 287 biological processes (BP), 54 cellular components (CC), and 79 molecular functions (MF). Through KEGG pathway analysis (Fig. 3G), we identified a total of 70 related pathways and selected the top 20 pathways based on significant enrichment for visual analysis. Through the combination of KEGG results from the literature, we selected RAGE signaling pathways for later molecular biology experiments.

Molecular Docking

In the PPI network, we selected high to moderate values for the targets HIF1A (PDB ID: 3HQU), Vascular Endothelial Growth Factor A (VEGFA) (PDB ID: 1BJ1), and Caspase-3 (PDB ID: 1NME). Within the AGEs-RAGE signaling pathway, the primary targets include AGEs (PDB ID: 2MOV), RAGE (PDB ID: 2E5E), NF-κB (PDB ID: 1A3Q), and IL-1β (PDB ID: 5BVJ). Key targets of the NRF2 signaling pathway are NRF2 (PDB ID: 2FLU), kelch-like ECH-associated protein 1 (Keap1) (PDB ID: 4IFJ), and heme oxygenase-1 (HO-1) (PDB ID: 4L9K). Additionally, synaptic proteins related to PSD95 (PDB ID: 8AH4) and SYP (AlphaFold ID: AF-P08247-F1) were included for molecular docking (Fig. 3H–S).

A molecular docking binding energy score of less than -5 was considered to indicate good binding ability. A molecular docking binding energy score of less than -7 was considered to indicate strong binding ability. The results indicate that DMY exhibits a strong binding affinity for the target proteins. The docking scores, which illustrate the molecular docking outcomes, are presented in Fig. 3T.

The Targets with Higher PPI Degree Values of DMY had a Tendency to Change in the Rats with Depression

Compared to the control group, the depression model group exhibited a marked reduction in VEGFA protein expression, accompanied by significantly elevated levels of Caspase-3 and HIF1A. After the DMY treatment, VEGFA expression increased a lot when compared to model group. Simultaneously, Caspase-3 and HIF1A expression were declined (Fig. 4A–F) (n = 4, $p < 0.05$).

Effect of DMY on AGEs-RAGE Signaling in the Rats with Depression

This study adopted Western blotting and immunohistochemistry to detect the levels of proteins associated with the AGEs-RAGE signaling pathway, aiming to explore the role of DMY in depressive behavior in a rat model of depression as well as its mechanism of action. Our results revealed that, compared to the control group, there was significant down—regulation of AGEs, RAGE, NF-κB, and IL-1β in the depressed rats treated with DMY (Fig. 4G–P) (n = 4, $p < 0.05$). The results demonstrated that DMY inhibited the AGEs-RAGE signaling pathway, thereby improving depressive behavior.

Effect of DMY on NRF2 Signaling in the Depression Rats

Immunofluorescence Dihydroethidium (DHE) Results

The model group demonstrated significantly higher DHE intensity in both the cerebral cortex ($p < 0.001$) and the hippocampus ($p < 0.01$) compared to the control group. In comparison, the 40 mg/kg DMY and 80 mg/kg DMY group were lower than the model group in both the cerebral cortex ($p < 0.001$) and hippocampus ($p < 0.01$). DMY significantly reduced oxidative stress levels in the rat cerebral cortex and hippocampus (Fig. 5A–D) (n = 4).

Western Blot Detection NRF2 Signaling Pathway

The results obtained from Western blotting and immunohistochemistry indicated that the levels of NRF2 and HO-1 proteins were significantly lower in the model group compared to the control group, while it was increased by the DMY treatment group. Additionally, the expression of Keap1 was found to be significantly elevated in this model, while it was attenuated by the DMY treatment group (Fig. 5E–L) (n = 4, $p < 0.05$).

Transmission Electron Microscope (TEM)

Within the control group, the synaptic structure was complete; the quantity of synapses was high, and the synaptic vesicles were numerous, round, and clear. In the group subjected to the depression model, the synaptic structure was unclear, and the synapses and synaptic vesicles were fewer in number. The synaptic architecture in the DMY group group exhibited structural integrity, with synaptic density and vesicle counts surpassing those observed in the model group, yet remaining marginally lower than control levels. A significant decrease in the expression of SYP and PSD95 proteins was observed in the model group. This situation

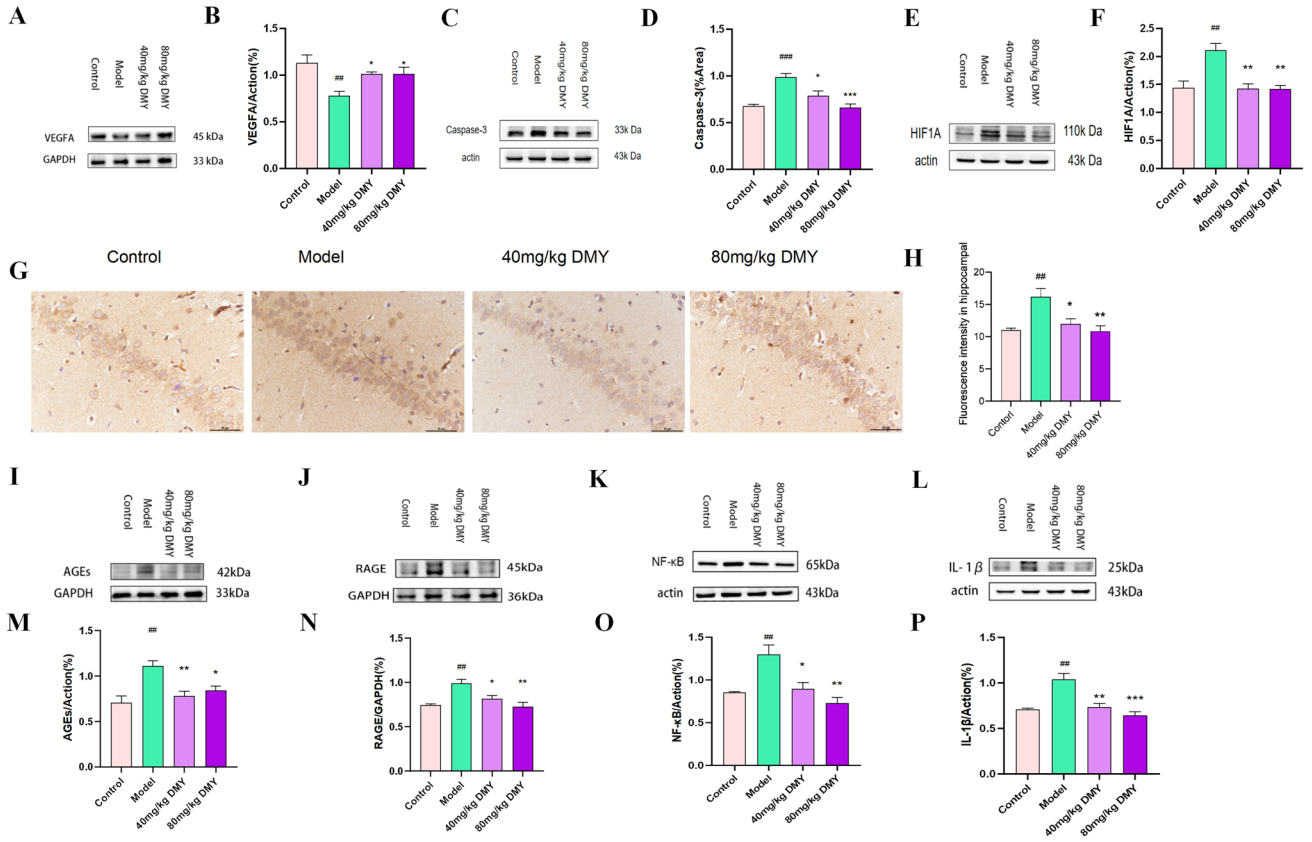

Fig. 4 **A**, **B**: VEGFA western blot bands and expression; **C**, **D**: Caspase-3 western blot bands and expression; **E**, **F**: HIF1A western blot bands and expression. **G**: Immunofluorescence for NF-κB in hippocampus; **H**: The area of NF-κB-positive cells in the hippocampus. **I**, **J**: AGEs western blot bands and expression. **K**, **L**: RAGE western blot bands and expression. **M**, **N**: NF-κB western blot bands and expression. **O**, **P**: IL-1β western blot bands and expression. All data are expressed as Mean ± SEM (n = 4 tissue samples). $^{\#\#}p < 0.01$ and $^{\#\#\#}p < 0.001$ vs.control, $^{*}p < 0.05$, $^{**}p < 0.01$, and $^{***}p < 0.01$ vs. model

was overturned by DMY (Fig. 5M–Q) (TEM: n = 2; Western blotting: n = 4, $p < 0.05$).

Materials and Methods

Animals and Groups

Fifty SD rats, specific pathogen-free (SPF) grade, aged 6 weeks (weighing 200–220 g), were obtained from Liaoning Changsheng Biological Co. The study was approved by the Animal Ethics Committee of Shenyang Medical College (approval number: SYYXY2023021801).The animals were raised in an environment with a standard 12 h-12 h light/dark cycle and had free access to food and water. Humidity levels were maintained between 50 and 60%, while the temperature was consistently regulated at 23 °C.

Adhering to the principle of equal numbers of male and female rats, the subjects were divided into five groups through random assignment: control, depression model, depression model + low-dose DMY (40 mg/kg), depression model + high-dose DMY (80 mg/kg), and depression model + fluoxetine (2 mg/kg). From the initial day of the CUMS combined with social isolation modeling, the administration method was gavage. The administration persisted throughout the entire experimental period, lasting 56 days during the gavage cycle. DMY (HPLC purity > 98%, Chengdu Pufei De Biotech Co., Ltd) was dissolved in saline. All procedures were carried out in accordance with the Chinese Animal Welfare Law and the guidelines of the Animal Ethics Committee of Shenyang Medical College.The experimental procedure is depicted in Fig. 1.

Animal Models Were Established

Rats were randomly assigned to a 42-day chronic variable stress protocol, which including 24-h water deprivation, 24-h fasting, tail clamping, light–dark reversal, 4-h restraint, 4-h damp bedding, 4-h cage tilting, and forced swimming in cold water at 4 °C for 5 min. These eight stress factors were randomly applied within 42 days with one stimulus per day and were not repeated within 3 days to prevent predictability.

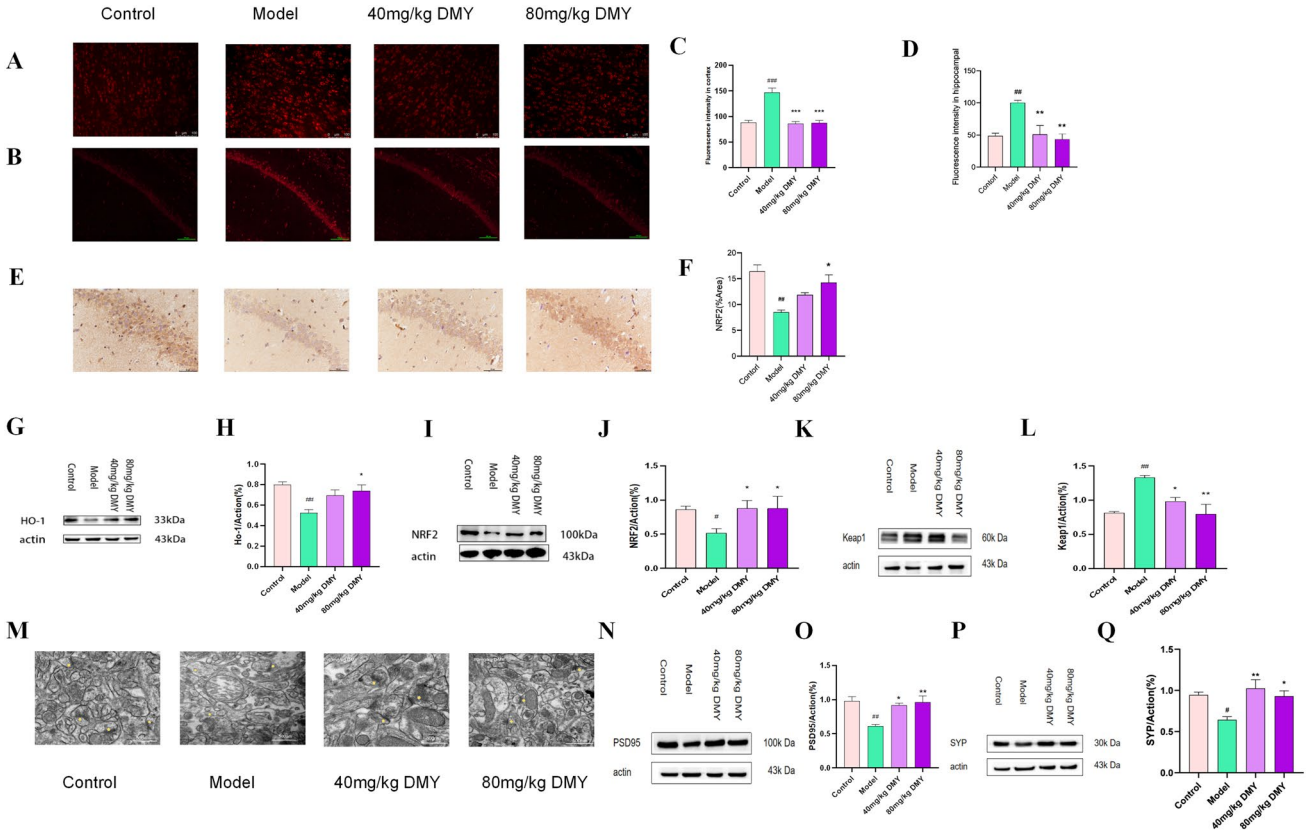

Fig. 5 **A**, **B**: Images of DHE staining in the cortex and hippocampus; **C**: cortex DHE average fluorescence intensity analysis; **D**: hippocampus DHE average fluorescence intensity analysis. **E**: Images of NRF2 immunofluorescence in the hippocampus; **F**: The area of NRF2-positive cells in the hippocampus. **G**, **H**: HO-1 western blot bands and expression. **I**, **J**: NRF2 western blot bands and expression. **K**, **L**: Keap1 western blot bands and expression. **M**: The scale bar in the representative image of synaptic morphology is 500 nm. **N**, **O**: PSD95 western blot bands and expression. **P**, **Q**: SYP western blot bands and expression. TEM data are presented as n = 2 rats, while other data are expressed as Mean ± SEM (n = 4 tissue samples). $^{\#}p < 0.01$, $^{\#\#}p < 0.01$, and $^{\#\#\#}p < 0.001$ vs.control; $^{*}p < 0.05$, $^{**}p < 0.01$ and $^{***}p < 0.001$ vs. model

Meanwhile, the rats were subjected to 42—day social isolation. The control group was group-housed under normal conditions.

Behavior Tests

OFT

All groups underwent behavioral testing under identical conditions. The OFT was performed as follows: every rat was positioned in the same corner of the arena for a 1-min acclimatization period, followed by a 5-min recording of spontaneous activity. The time spent and distance traveled within the central area were utilized to evaluate anxiety-like behaviors [40]. Following each experiment, the bottom and inner walls of each rat's active area were cleaned, and 0.1% benzalkonium chloride was sprayed to eliminate any odors that could disturb other rats.

Y-Maze

At the beginning of the trial, the rats were placed in arm A with their backs in the Y-maze (arm A served as the designated starting point). This prevented the subjects from observing the entire experimental setup and granted free access to all three arms. Record the sequence of entries into the three arms and the total number of arm entries within a 5-min interval. The correct alternation response was defined as entering three distinct arms consecutively. This offered an assessment of the spatial working memory capabilities in the rats. The spontaneous alternation rate was computed as [Number of Valid Alternations / (Total Arm Entries − 2)] × 100% [41]. Following each trial [42], it was imperative to thoroughly cleanse any residual waste from the Y-maze and disinfect it with 0.1% benzalkonium chloride to prevent persistent odors from impacting subsequent rat testing.

MCM Test

The MCM serves as a behavioral instrument independently developed by our laboratory. The device has a cylindrical structure measuring 200 cm in diameter and 80 cm in height. The MCM has been confirmed to detect anxiety and depression-like states in depressed rats [43]. It comprises six zones labeled A-F, with each housing a fan-shaped partition. Each fan-shaped partition is evenly distributed with four freely accessible or closed doorways, numbered 1–4, and the chassis has a rotating function. The experiment was divided into 2 days, with fan wall 1 as the starting point and fan wall 6 as the endpoint. On the first day of the experiment, the purpose was to allow the rats to acclimate to their new surroundings. All doors of fan walls 1–6 were opened, allowing the rats to roam freely for a duration of 10 min. Following a 24-h period, the second day of the experiment was conducted, with doors 1 and 4 of fan walls 1 to 6 opened and doors 2 and 3 closed. The rats explored the maze autonomously during a five-minute observation period. On the second day of the experiment, the distance moved and activity of the rats were recorded to determine the degree of depression. The experimental design of the MCM is shown in Fig. 2A, B.

SPT

Both containers were filled with a 1% sucrose water on the first day one to acclimate the animals to the sugar liquids [44]. The following day, each enclosure received one container of 1% sucrose water, and another container containing pure water. On the third day, a full day of continuous fasting and water deprivation was provided. On the fourth day, each enclosure received a 200 mL bottle of 1% sucrose water and another containing 200 mL of pure water, with their positions swapped to avoid location bias. After 4 h, both bottles were taken out and assessed to determine the consumption levels of sucrose water, pure water, and total intake. Sucrose preference ratio = (sucrose water consumption/total intake) × 100%.

NSFT

The rats underwent a 24-h fasting period where they had access to water only [45]. The rats were positioned in the corner of the test box with their backs to the wall. A number of pellets of comparable size were positioned at the center of the test box. Simultaneously, the feeding latency was measured as the time from when each animal was introduced into the test box until it began to ingest food. The experiment lasted for 5 min. During this period, "feeding" was defined as when an animal commenced chewing on the food and did not include instances where animals merely smelled or played with it before consuming.

FST

We conducted the FST in two days [46]. On the first day, the rats were acclimated to the environment for 15-min. The second day, the 6-min FST was performed as a behavioral assessment for depression-like animal models.

Network Pharmacology

Acquisition of Targets Related to DMY

Using the CAS number of DMY on the PubChem platform, we obtained its chemical structural formula. The targets were identified through the utilization of the TCMSP, TCMID, and Swiss Target Prediction databases.

Acquisition of Targets Related to Depression

Depression-related targets were sourced from the GeneCards, OMIM, PharmGKB, TTD, and DrugBank databases. After removing duplicate values, the targets related to depression were ultimately selected from the five databases.

Construction of PPI Network

The corresponding targets of DMY and depression-related targets were imported into the Venny 2.1.0 website to take the intersection and draw a Venn diagram. Common targets identified through Venn analysis were mapped onto the STRING platform as candidate anti-depressant targets of DMY, followed by PPI network generation. The PPI results were obtained from the STRING database and subsequently imported into Cytoscape version 3.8.0 to conduct a comprehensive analysis of network topology.

GO and KEGG Enrichment Analysis

The PPI network diagram was generated using the STRING database platform. DAVID (https://david.ncifcrf.gov/) was used for GO and KEGG enrichment analyses of overlapping targets. The results were presented visually through the Microscopic Letter website.

Molecular Docking

Based on the above experiments, we identified the key target protein of DMY, which was subsequently chosen as the receptor protein for molecular docking studies. The target protein was initially identified using the UniProt database, followed by retrieval of the corresponding file structure from the PDB and PubChem websites. Subsequently, PyMOL 2.4 software was employed for molecular visualization, while ChemDraw20 3D software utilized the FFMM90 force field

for energy minimization of the ligand molecules. AutoDockTools 1.5.6 was responsible for handling the preparation and docking procedures. AutoDock Vina version 1.1.2 was employed to perform molecular docking simulations aimed at further exploring the interactions between the target protein and the ligand model. The binding site characterized by the highest binding affinity to the target protein was identified for analysis. Visualization of the results was accomplished using PyMOL version 2.4 software.

Western Blotting Analysis

The hippocampal tissue was lysed in freshly prepared lysis buffer (Solarbio), and 1 mL of freshly prepared lysis buffer was added to each 0.1 g of fresh tissue. The homogenate was homogenized at a low temperature using a high-throughput homogenizer. Post homogenization, the homogenate was centrifuged at 12,000 × g at 4 °C for 15 min. The primary antibodies detected by Western blot included Caspase-3 (Cell Signaling Technology, 1:1000), NRF2 (Proteintech, 1:800), Keap1 (Proteintech, 1:1000), HO-1 (ABclonal, 1:800), VEGFA (Proteintech, 1:800), HIF1A (ZEN-BIOSCIENCE, 1:600), AGEs (Bioss, 1:300), RAGE (R&D Systems, 1:1000), IL-1β (Abcam, 1:1000), NF-κB (Abcam, 1:1000), and HRP-labeled secondary antibody (Proteintech, 1:4000) was used to detect specific protein bands on the membrane. Protein expression was analyzed utilizing enhanced chemiluminescence (ECL; Ncm ECL Ultra Kit; New Cell Molecular Biotechnology Co., China).

Immunofluorescence

Superoxide anion detection using the fluorescent probe DHE: For paraffin-embedded tissue sections, dewaxing and hydration were performed according to standard protocols. Each tissue section was incubated with 50 µL of 10 µmol/L DHE at 26 °C in the dark for 30 min. After incubation, the sections were mounted with antifluorescence quenching mounting medium. Fluorescence microscopic imaging was performed to visualize and document tissue section morphology.

TEM

After the brain slices were cut with a blade, the amygdala region of the rats was removed and sent to the university's electron microscope center for fixation, dehydration, heavy metal staining, and imaging. TEM observations were conducted to analyze the number of synapses and the morphological structure of the amygdala in rats.

Immunohistochemistry

The intact rat brain, after cardiac perfusion, was immersed in 4% paraformaldehyde fixative for 48–72 h. The fixed brain was then cut into 3–4 mm-thick slices using a brain matrix and placed in tissue cassettes for standby. After tissue fixation, the samples were embedded and sectioned. The sections were then subjected to deparaffinization and rehydration, followed by antigen retrieval and blocking. The sections were incubated overnight with rabbit anti-NF-κB antibody (Abcam, 1:500) and rabbit anti-NRF2 antibody (Proteintech, 1:800). The following day, secondary antibody incubation was conducted for 50 min, after which 3,3′-Diaminobenzidine (DAB) staining was applied. The sections were subsequently mounted and examined under a microscope.

Statistical Analysis

The data were presented as the mean ± standard error of the mean (SEM). The differences between groups were analyzed by repeated one-way analysis of variance (ANOVA), and non-parametric tests were used for data not conforming to normality, followed by Fisher's least significant difference (LSD) multiple comparisons test, with a significance level set at $p < 0.05$. The analysis of the data was conducted using SPSS version 20.0.

Discussion

Depression is a common and recurrent psychiatric disease that imposes a heavy economic burden on society. Currently, there are several hypotheses regarding the mechanism of depression. However, the exact mechanism has not been completely elucidated. The inflammation and cytokine hypothesis is a widely accepted mechanism for the pathogenesis of depression [47]. Studies suggest that immune abnormalities, particularly inflammation, are closely associated with depression. Anti-inflammatory therapy may become the focus in the treatment of depression [48]. From a modern pharmacological perspective, DMY is known for its anti-tumor, anti-microbial, blood lipid-regulating, liver-protective, cardiovascular, nervous system-protective, anti-inflammatory, antioxidant, and several other pharmacological effects and developments [49].

CUMS is an internationally recognized model of classical depression. Since it was first proposed in 1982 [50], it has been widely recognized for its ability to induce depression-like behavior through relatively mild and unpredictable artificial stimuli. This model is extensively used because it closely resembles the pathological mechanisms of human depression. To further optimize the model, this study integrated social isolation. According to the relevant literature,

CUMS combined with social isolation can more effectively facilitate the establishment of animal models of depression [51]. Depression has two major behavioral manifestations: anhedonia and behavioral despair [52]. Modeling rats not only demonstrated these characteristics but also showed decreased exploration and motor activity. This mirrors the reduction in energy levels and cognitive impairments commonly seen in individuals diagnosed with depression. Evaluation of the effectiveness of antidepressant drugs in animal models requires a variety of assessment methods. A single method is not sufficient to completely reflect the actual situation. Therefore, the integrated OFT, SPT, FST, and NSFT was employed to assess the behavior of the rats.

The OFT was used to detect anxiety-like behavioral changes in depressed rats by observing the activity time and moving distance of the central region. The results demonstrated that the model group was significantly lower than the control group on the two indices. However, the DMY and fluoxetine groups demonstrated the opposite trend. In the Y-maze, we counted the total arm entries (reflecting exploratory and motor abilities) and the spontaneous alternating response rate (reflecting spatial memory ability) in depressed rats. Y-maze results demonstrated that DMY improved exploration and motor function in depressed rats. Nevertheless, the five groups showed no significant differences in the spontaneous alternating response rate, indicating that there were no differences in spatial memory among the five groups. The reduced distance and activity observed in the model group were increased in the DMY group, and this reversal was further corroborated using a MCM. The hot zone trace diagram and trajectory analysis showed that the control group exhibited extensive activity with uniform distribution. The model group had less activity and uneven distribution, while the DMY group demonstrated greater activity and more uniform distribution than the model group. Following the completion of the OFT, Y-maze, and MCM, the NSFT, SPT, and FST were subsequently employed to assess the behavioral responses of rats.

The NSFT is a valuable tool for assessing the efficacy of antidepressant medications and examining anxiety-like behaviors in animal models of depression [53]. The experiment was grounded in the interplay between the feeding motivation observed in rodents and their apprehension in unfamiliar surroundings [54]. The results showed that DMY significantly shortened the feeding latency of model rats, suggesting that it may serve as a potential component of antidepressant medications. The SPT is designed according to the preferences of rodents for sweetness and is used to evaluate the most effective way to lose sensation in rats [27]. The SPT was used to detect two indicators: pure water consumption and sucrose preference ratio. In the experimental group, rats fed pure water did not demonstrate a statistically significant difference, which is different from the findings of previous studies [55]. Notably, DMY significantly increased the sucrose preference ratio in depressed rats, suggesting that it may improve anhedonia associated with depression. The FST is also known as the behavioral despair experiment, where animals cannot escape despair caused by bad environmental behavior. It is one of the most classic methods for assessing depression-like behaviors in animals. In the FST, DMY significantly improves depression-like behaviors in model group.

Through database mining, potential targets of DMY and depression-related targets were systematically identified. In this study, DMY targets and depression-related targets were retrieved from a database. By taking the intersection of these two target sets and predicting potential targets for DMY's anti-depressive effects, we identified 79 potential anti-depression targets of DMY. The specific mechanisms need to be further explored. In the PPI analysis, we selected high-degree targets, including Caspase-3, VEGFA, and HIF1A. Subsequent molecular docking experiments verified that these proteins exhibited significant binding affinity to DMY. To further validate our findings, Western blot experiments were conducted. The results indicated a significant increase in the expression levels of Caspase-3 and HIF1A proteins within the hippocampus of the depressed model group, while there was a notable decrease in VEGFA expression. However, these alterations were markedly influenced by the administration of DMY. Although the above findings suggest that Caspase-3, VEGFA, and HIF1A may be the key regulatory factors in depression, the exact interplay mechanism between them still needs to be explored in detail in future experiments. From the KEGG enrichment analysis, the AGEs-RAGE signaling pathway was selected for further molecular studies based on a network pharmacology review of the relevant literature. AGEs are hyperoxic compounds that, when stimulated by high glucose, cause inflammation, aging, and oxidative stress, bind to their receptor RAGE, and initiate signaling pathways [56]. This study focused on the inflammatory aspects induced by AGEs [57] to verify whether DMY could improve depression-like behavior in rat models by reducing the inflammatory mechanism induced by AGEs. Molecular docking was conducted on the key proteins AGEs, RAGE, NF-κB, and IL-1β,which had strong binding ability to DMY. We verified AGEs-RAGE by Western blot experiments and Immunohistochemistry experiments to determine its expression trend in depression models. The findings from Western blot experiments and immunohistochemistry demonstrated that, when juxtaposed with the control group, the protein levels of AGEs, RAGE, NF-κB, and IL-1β in the depression model group exhibited a notable elevation. In contrast, dihydromyricetin (DMY) effectively mitigated these increases. These results strongly suggest that DMY has the potential to alleviate depressive symptoms by modulating the AGEs-RAGE signaling pathway.

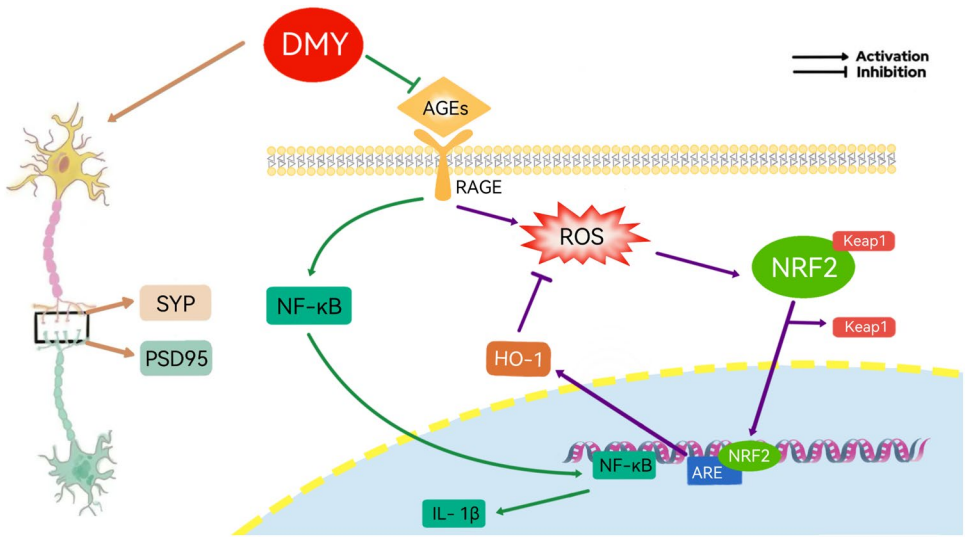

Fig. 6 Molecular mechanisms of DMY alleviates depression-like behavior in rats

An excessive buildup of oxidative stress can facilitate the formation of AGEs [13], which interact with their receptor RAGE. This leads to an enhancement in the activity of the NADPH oxidase family, resulting in the overproduction of ROS [58]. Based on these theories, we proposed the hypothesis that the AGEs-RAGE signaling pathway initiates the production of ROS,which in turn triggers oxidative stress responses [59]. NRF2 is one of the most classic oxidative stress pathways [60]. We hypothesized that DMY may improve depression-like changes in depressed rats by activating the NRF2 signaling pathway through AGEs-RAGE. Molecular docking demonstrated that NRF2, Keap1, and HO-1 exhibit strong binding affinity to DMY. We used a DHE fluorescent probe to detect ROS levels in the hippocampus and cortex of rats to examine the antioxidant effects of DMY in each group. The results demonstrated that DMY notably reduced the ROS levels in the hippocampus and cortex of rats with depression. Western blotting and immunohistochemistry experiments revealed that the expression of NRF2 and HO-1 significantly increased, while Keap1 expression was lower in the DMY group compared to the model group. These findings indicate that DMY alleviates depression-like behaviors in rats through the activation of the NRF2 signaling pathway.

We determined the impact of DMY on synaptic plasticity in depression model rats. The alterations in amygdala neurons in each group were observed using TEM. DMY significantly improved the synaptic ultrastructure in model rats. Among the mechanisms underlying depression pathogenesis, hippocampal neuroplasticity is vital. Neuroplasticity entails modifications across various brain regions, prominently including the prefrontal cortex, hippocampus, amygdala, and nucleus accumbens. These modifications lead to the dysfunction of brain nerve circuits and depression symptoms [61]. Antidepressant treatment can restore synaptic protein expression levels and improve synaptic plasticity [62]. SYP and PSD95 are important components of synaptic plasticity. Studies have demonstrated the severe depression model rat's hippocampal synaptic protein expression in the brain regions [15]. Through molecular docking and western blot experiments, we found that the synaptic proteins SYP and PSD95 have strong binding affinity for DMY and that DMY significantly enhanced the expression of PSD95 and SYP. These results suggested that DMY protected neurons and reduced neuronal damage by regulating synaptic plasticity, thereby alleviating depression. Molecular mechanisms by which DMY alleviates depression-like behavior in rats (Fig. 6).

In summary, the behavioral results demonstrated that DMY improved depression-like behavior in CUMS combined with social isolation-induced model rats. Network pharmacology and molecular biology have collaboratively demonstrated that DMY alleviates depression-like behavioral changes by inhibiting the AGEs-RAGE signaling pathway, activating the NRF2 signaling pathway, and regulating synaptic functions.

Acknowledgements This study received financial support from several sources, including the Liaoning Provincial Department of Education (SYYX202009), the Liaoning Provincial Department of Science and Technology (2021-MS-351), and the Science and Technology Innovation Project for Graduate Students at Shenyang Medical College (Y20220511).

Author Contributions Conceptualization by Ge Jin and Dafeng Bai; data curation, Xue Li, Decheng Wei, and Jiaqi Chen; formal analysis, Yuchuan Zhang, and Zitong Wang; Funding source provide,Ge Jin; investigation, Xioameng Duan and Yanzong Jiang; supervision, Ge Jin and Hui Jia; visualization, Miaoqi Chen and Decheng Wei; writing original draft, Xue Li and Miaoqi Chen; writing review and editing, Ge Jin. All authors have read and agreed to the published version of the manuscript.

Funding This study was supported by Department of Education of Liaoning Province, SYYX202009, Department of Science and Technology of Liaoning Province, 2021-MS-351.

Data Availability No datasets were generated or analysed during the current study.

Declarations

Competing interests The authors declare no competing interests.

References

1. Malhi GS, Mann JJ (2018) Depression. Lancet (London, England) 392(10161):2299–2312. https://doi.org/10.1016/s0140-6736(18)31948-2
2. De Hert M, Peuskens J (2006) Cost of disorders of the brain in Europe. Eur J Neurol 13(11):e7. https://doi.org/10.1111/j.1468-1331.2006.01388.x
3. Kessler RC, Angermeyer M, Anthony JC, Graaf RDE, Demyttenaere K, Gasquet I, Girolamo GDE, Gluzman S, Gureje O, Haro JM, Kawakami N, Karam A, Levinson D, Medina Mora ME, Oakley Browne MA, Posada-Villa J, Stein DJ, Adley Tsang CH, Aguilar-Gaxiola S, Alonso J, Lee S, Heeringa S, Pennell BE, Berglund P, Gruber MJ, Petukhova M, Chatterji S, Ustün TB (2007) Lifetime prevalence and age-of-onset distributions of mental disorders in the World Health Organization's World Mental Health Survey Initiative. World Psychiatry 6(3):168–176
4. Miret M, Ayuso-Mateos JL, Sanchez-Moreno J, Vieta E (2013) Depressive disorders and suicide: epidemiology, risk factors, and burden. Neurosci Biobehav Rev 37(10 Pt 1):2372–2374. https://doi.org/10.1016/j.neubiorev.2013.01.008
5. Frank E, Thase ME (1999) Natural history and preventative treatment of recurrent mood disorders. Annu Rev Med 50:453–468. https://doi.org/10.1146/annurev.med.50.1.453
6. Daviu N, Bruchas MR, Moghaddam B, Sandi C, Beyeler A (2019) Neurobiological links between stress and anxiety. Neurobiol Stress 11:100191. https://doi.org/10.1016/j.ynstr.2019.100191
7. Maes M, Vandoolaeghe E, Ranjan R, Bosmans E, Bergmans R, Desnyder R (1995) Increased serum interleukin-1-receptor-antagonist concentrations in major depression. J Affect Disord 36(1–2):29–36. https://doi.org/10.1016/0165-0327(95)00049-6
8. Huang C, Zhang F, Li P, Song C (2022) Low-dose IL-2 attenuated depression-like behaviors and pathological changes through restoring the balances between IL-6 and TGF-β and between Th17 and Treg in a chronic stress-induced mouse model of depression. Int J Mol Sci. https://doi.org/10.3390/ijms232213856
9. Li R, Zhao D, Qu R, Fu Q, Ma S (2015) The effects of apigenin on lipopolysaccharide-induced depressive-like behavior in mice. Neurosci Lett 594:17–22. https://doi.org/10.1016/j.neulet.2015.03.040
10. Zhou M, Zhang Y, Shi L, Li L, Zhang D, Gong Z, Wu Q (2024) Activation and modulation of the AGEs-RAGE axis: implications for inflammatory pathologies and therapeutic interventions - a review. Pharmacol Res 206:107282. https://doi.org/10.1016/j.phrs.2024.107282
11. Kontis D, Boulougouris V, Papakosta VM, Kalogerakou S, Papadopoulos S, Poulopoulou C, Papadimitriou GN, Tsaltas E (2008) Dopaminergic and serotonergic modulation of persistent behaviour in the reinforced spatial alternation model of obsessive-compulsive disorder. Psychopharmacology 200(4):597–610. https://doi.org/10.1007/s00213-008-1241-5
12. Reddy VP, Aryal P, Darkwah EK (2022) Advanced glycation end products in health and disease. Microorganisms. https://doi.org/10.3390/microorganisms10091848
13. Koska J, Saremi A, Howell S, Bahn G, De Courten B, Ginsberg H, Beisswenger PJ, Reaven PD (2018) Advanced glycation end products, oxidation products, and incident cardiovascular events in patients with type 2 diabetes. Diabetes Care 41(3):570–576. https://doi.org/10.2337/dc17-1740
14. Yang T, Nie Z, Shu H, Kuang Y, Chen X, Cheng J, Yu S, Liu H (2020) The role of BDNF on neural plasticity in depression. Front Cell Neurosci 14:82. https://doi.org/10.3389/fncel.2020.00082
15. Jiang L, Zhang H, Zhou J, Tang X, Luo L, Huang P, Yi W, Xu N, Liu J, Fu W (2020) Involvement of hippocampal AMPA receptors in electroacupuncture attenuating depressive-like behaviors and regulating synaptic proteins in rats subjected to chronic unpredictable mild stress. World Neurosurg 139:e455–e462. https://doi.org/10.1016/j.wneu.2020.04.042
16. Liu C, Zhao Y, Zhao WJ (2024) Positive effect of 6-gingerol on functional plasticity of microglia in a rat model of LPS-induced depression. J Neuroimmune Pharmacol 19(1):20. https://doi.org/10.1007/s11481-024-10123-z
17. Ren F, Guo R (2021) Synaptic microenvironment in depressive disorder: insights from synaptic plasticity. Neuropsychiatr Dis Treat 17:157–165. https://doi.org/10.2147/ndt.S268012
18. Chen S, Zhao X, Wan J, Ran L, Qin Y, Wang X, Gao Y, Shu F, Zhang Y, Liu P, Zhang Q, Zhu J, Mi M (2015) Dihydromyricetin improves glucose and lipid metabolism and exerts anti-inflammatory effects in nonalcoholic fatty liver disease: a randomized controlled trial. Pharmacol Res 99:74–81. https://doi.org/10.1016/j.phrs.2015.05.009
19. Li X, Yang ZS, Cai WW, Deng Y, Chen L, Tan SL (2021) Dihydromyricetin inhibits tumor growth and epithelial-mesenchymal transition through regulating miR-455-3p in cholangiocarcinoma. J Cancer 12(20):6058–6070. https://doi.org/10.7150/jca.61311
20. Shi J, Peng X, Huang J, Zhang M, Wang Y (2025) Dihydromyricetin alleviated acetaminophen-induced acute kidney injury via Nrf2-dependent anti-oxidative and anti-inflammatory effects. Int J Mol Sci. https://doi.org/10.3390/ijms26052365
21. Dong S, Zhu M, Wang K, Zhao X, Hu L, Jing W, Lu H, Wang S (2021) Dihydromyricetin improves DSS-induced colitis in mice via modulation of fecal-bacteria-related bile acid metabolism. Pharmacol Res 171:105767. https://doi.org/10.1016/j.phrs.2021.105767
22. Feng J, Wang JX, Du YH, Liu Y, Zhang W, Chen JF, Liu YJ, Zheng M, Wang KJ, He GQ (2018) Dihydromyricetin inhibits microglial activation and neuroinflammation by suppressing NLRP3 inflammasome activation in APP/PS1 transgenic mice. CNS Neurosci Ther 24(12):1207–1218. https://doi.org/10.1111/cns.12983
23. Ren ZX, Zhao YF, Cao T, Zhen XC (2016) Dihydromyricetin protects neurons in an MPTP-induced model of Parkinson's disease by suppressing glycogen synthase kinase-3 beta activity. Acta Pharmacol Sin 37(10):1315–1324. https://doi.org/10.1038/aps.2016.42
24. Getachew B, Csoka AB, Copeland RL, Manaye KF, Tizabi Y (2023) Dihydromyricetin protects against salsolinol-induced toxicity in dopaminergic cell line: implication for parkinson's disease. Neurotox Res 41(2):141–148. https://doi.org/10.1007/s12640-022-00631-2
25. Watanabe S, Omran AA, Shao AS, Xue C, Zhang Z, Zhang J, Davies DL, Shao XM, Watanabe J, Liang J (2022) Dihydromyricetin improves social isolation-induced cognitive impairments and astrocytic changes in mice. Sci Rep 12(1):5899. https://doi.org/10.1038/s41598-022-09814-5

26. Willner P (1984) The validity of animal models of depression. Psychopharmacology 83(1):1–16. https://doi.org/10.1007/bf00427414
27. Ma XC, Jiang D, Jiang WH, Wang F, Jia M, Wu J, Hashimoto K, Dang YH, Gao CG (2011) Social isolation-induced aggression potentiates anxiety and depressive-like behavior in male mice subjected to unpredictable chronic mild stress. PLoS ONE 6(6):e20955. https://doi.org/10.1371/journal.pone.0020955
28. Jiang H, Zhang X, Lu J, Meng H, Sun Y, Yang X, Zhao B, Bao T (2018) Antidepressant-like effects of acupuncture-insights from DNA methylation and histone modifications of brain-derived neurotrophic factor. Front Psych 9:102. https://doi.org/10.3389/fpsyt.2018.00102
29. Wang M, Bi Y, Zeng S, Liu Y, Shao M, Liu K, Deng Y, Wen G, Sun X, Zeng P, Jing L, Lv Z (2019) Modified Xiaoyao San ameliorates depressive-like behaviors by triggering autophagosome formation to alleviate neuronal apoptosis. Biomed Pharmacother 111:1057–1065. https://doi.org/10.1016/j.biopha.2018.12.141
30. Zhang Z, Fei P, Mu J, Li W, Song J (2014) Hippocampal expression of aryl hydrocarbon receptor nuclear translocator 2 and neuronal PAS domain protein 4 in a rat model of depression. Neurol Sci 35(2):277–282. https://doi.org/10.1007/s10072-013-1505-7
31. Ru J, Li P, Wang J, Zhou W, Li B, Huang C, Li P, Guo Z, Tao W, Yang Y, Xu X, Li Y, Wang Y, Yang L (2014) TCMSP: a database of systems pharmacology for drug discovery from herbal medicines. J Cheminform 6:13. https://doi.org/10.1186/1758-2946-6-13
32. Daina A, Michielin O, Zoete V (2019) SwissTargetPrediction: updated data and new features for efficient prediction of protein targets of small molecules. Nucleic Acids Res 47(W1):W357-w364. https://doi.org/10.1093/nar/gkz382
33. Wang X, Shen Y, Wang S, Li S, Zhang W, Liu X, Lai L, Pei J, Li H (2017) PharmMapper 2017 update: a web server for potential drug target identification with a comprehensive target pharmacophore database. Nucleic Acids Res 45(W1):W356-w360. https://doi.org/10.1093/nar/gkx374
34. Rebhan M, Chalifa-Caspi V, Prilusky J, Lancet D (1997) GeneCards: integrating information about genes, proteins and diseases. Trends Genet 13(4):163. https://doi.org/10.1016/s0168-9525(97)01103-7
35. Amberger JS, Bocchini CA, Schiettecatte F, Scott AF, Hamosh A (2015) OMIM.org: Online Mendelian Inheritance in Man (OMIM®), an online catalog of human genes and genetic disorders. Nucleic Acids Res. https://doi.org/10.1093/nar/gku1205
36. Whirl-Carrillo M, McDonagh EM, Hebert JM, Gong L, Sangkuhl K, Thorn CF, Altman RB, Klein TE (2012) Pharmacogenomics knowledge for personalized medicine. Clin Pharmacol Ther 92(4):414–417. https://doi.org/10.1038/clpt.2012.96
37. Zhou Y, Zhang Y, Zhao D, Yu X, Shen X, Zhou Y, Wang S, Qiu Y, Chen Y, Zhu F (2024) TTD: therapeutic target database describing target druggability information. Nucleic Acids Res 52(D1):D1465-d1477. https://doi.org/10.1093/nar/gkad751
38. Knox C, Wilson M, Klinger CM, Franklin M, Oler E, Wilson A, Pon A, Cox J, Chin NEL, Strawbridge SA, Garcia-Patino M, Kruger R, Sivakumaran A, Sanford S, Doshi R, Khetarpal N, Fatokun O, Doucet D, Zubkowski A, Rayat DY, Jackson H, Harford K, Anjum A, Zakir M, Wang F, Tian S, Lee B, Liigand J, Peters H, Wang RQR, Nguyen T, So D, Sharp M, da Silva R, Gabriel C, Scantlebury J, Jasinski M, Ackerman D, Jewison T, Sajed T, Gautam V, Wishart DS (2024) DrugBank 6.0: the DrugBank knowledgebase for 2024. Nucleic Acids Res. https://doi.org/10.1093/nar/gkad976
39. Szklarczyk D, Gable AL, Lyon D, Junge A, Wyder S, Huerta-Cepas J, Simonovic M, Doncheva NT, Morris JH, Bork P, Jensen LJ, Mering CV (2019) STRING v11: protein-protein association networks with increased coverage, supporting functional discovery in genome-wide experimental datasets. Nucleic Acids Res 47(D1):D607-d613. https://doi.org/10.1093/nar/gky1131
40. Prut L, Belzung C (2003) The open field as a paradigm to measure the effects of drugs on anxiety-like behaviors: a review. Eur J Pharmacol 463(1–3):3–33. https://doi.org/10.1016/s0014-2999(03)01272-x
41. Li M, Zhang J, Chen W, Liu S, Liu X, Ning Y, Cao Y, Zhao Y (2023) Supraphysiologic doses of 17β-estradiol aggravate depression-like behaviors in ovariectomized mice possibly via regulating microglial responses and brain glycerophospholipid metabolism. J Neuroinflamm 20(1):204. https://doi.org/10.1186/s12974-023-02889-5
42. Jin G, Bai D, Yin S, Yang Z, Zou D, Zhang Z, Li X, Sun Y, Zhu Q (2016) Silibinin rescues learning and memory deficits by attenuating microglia activation and preventing neuroinflammatory reactions in SAMP8 mice. Neurosci Lett 629:256–261. https://doi.org/10.1016/j.neulet.2016.06.008
43. Cao G, Wei X, Li W, Yin H, Lang W, Wei P, Zhu Q, Jin G (2021) Verification of a multi-function closed maze for the detection of affective disorder and spatial cognitive impairment in post-weaning socially isolated rats. Neurosci Lett 763:136192. https://doi.org/10.1016/j.neulet.2021.136192
44. Markov DD (2022) Sucrose preference test as a measure of anhedonic behavior in a chronic unpredictable mild stress model of depression: outstanding issues. Brain Sci. https://doi.org/10.3390/brainsci12101287
45. Blasco-Serra A, González-Soler EM, Cervera-Ferri A, Teruel-Martí V, Valverde-Navarro AA (2017) A standardization of the novelty-suppressed feeding test protocol in rats. Neurosci Lett 658:73–78. https://doi.org/10.1016/j.neulet.2017.08.019
46. Slattery DA, Cryan JF (2012) Using the rat forced swim test to assess antidepressant-like activity in rodents. Nat Protoc 7(6):1009–1014. https://doi.org/10.1038/nprot.2012.044
47. Kohler O, Krogh J, Mors O, Benros ME (2016) Inflammation in depression and the potential for anti-inflammatory treatment. Curr Neuropharmacol 14(7):732–742. https://doi.org/10.2174/1570159x14666151208113700
48. Miller AH, Maletic V, Raison CL (2009) Inflammation and its discontents: the role of cytokines in the pathophysiology of major depression. Biol Psychiat 65(9):732–741. https://doi.org/10.1016/j.biopsych.2008.11.029
49. Zhang J, Chen Y, Luo H, Sun L, Xu M, Yu J, Zhou Q, Meng G, Yang S (2018) Recent update on the pharmacological effects and mechanisms of dihydromyricetin. Front Pharmacol 9:1204. https://doi.org/10.3389/fphar.2018.01204
50. Katz RJ, Sibel M (1982) Further analysis of the specificity of a novel animal model of depression–effects of an antihistaminic, antipsychotic and anxiolytic compound. Pharmacol Biochem Behav 16(6):979–982. https://doi.org/10.1016/0091-3057(82)90056-9
51. Su GY, Yang JY, Wang F, Ma J, Zhang K, Dong YX, Song SJ, Lu XM, Wu CF (2014) Antidepressant-like effects of Xiaochaihutang in a rat model of chronic unpredictable mild stress. J Ethnopharmacol 152(1):217–226. https://doi.org/10.1016/j.jep.2014.01.006
52. Hales CA, Stuart SA, Anderson MH, Robinson ES (2014) Modelling cognitive affective biases in major depressive disorder using rodents. Br J Pharmacol 171(20):4524–4538. https://doi.org/10.1111/bph.12603
53. Bodnoff SR, Suranyi-Cadotte B, Aitken DH, Quirion R, Meaney MJ (1988) The effects of chronic antidepressant treatment in an animal model of anxiety. Psychopharmacology 95(3):298–302. https://doi.org/10.1007/bf00181937
54. Richardson-Jones JW, Craige CP, Guiard BP, Stephen A, Metzger KL, Kung HF, Gardier AM, Dranovsky A, David DJ, Beck SG, Hen R, Leonardo ED (2010) 5-HT1A autoreceptor levels determine vulnerability to stress and response to antidepressants.

Neuron 65(1):40–52. https://doi.org/10.1016/j.neuron.2009.12.003
55. Liu X, Jin G, Fan B, Xing Y, Wang L, Wang M, Yuan Y, Zhu Q (2018) The impact of ALDH2 activation by Alda-1 on the expression of VEGF in the hippocampus of a rat model of post-MI depression. Neurosci Lett 674:156–161. https://doi.org/10.1016/j.neulet.2018.03.048
56. Lin JA, Wu CH, Lu CC, Hsia SM, Yen GC (2016) Glycative stress from advanced glycation end products (AGEs) and dicarbonyls: an emerging biological factor in cancer onset and progression. Mol Nutr Food Res 60(8):1850–1864. https://doi.org/10.1002/mnfr.201500759
57. Matsui T, Yamagishi S, Takeuchi M, Ueda S, Fukami K, Okuda S (2010) Nifedipine inhibits advanced glycation end products (AGEs) and their receptor (RAGE) interaction-mediated proximal tubular cell injury via peroxisome proliferator-activated receptor-gamma activation. Biochem Biophys Res Commun 398(2):326–330. https://doi.org/10.1016/j.bbrc.2010.06.093
58. Zhou Q, Xu H, Zhao Y, Liu B, Cheng KW, Chen F, Wang M (2022) 6-C-(E-Phenylethenyl)-naringenin, a styryl flavonoid, inhibits advanced glycation end product-induced inflammation by upregulation of Nrf2. J Agric Food Chem 70(12):3842–3851. https://doi.org/10.1021/acs.jafc.2c00163
59. Zhang Z, Yang H, Yang J, Xie J, Xu J, Liu C, Wu C (2019) Pseudoginsenoside-F11 attenuates cognitive impairment by ameliorating oxidative stress and neuroinflammation in d-galactose-treated mice. Int Immunopharm 67:78–86. https://doi.org/10.1016/j.intimp.2018.11.026
60. Di Meo S, Reed TT, Venditti P, Victor VM (2016) Role of ROS and RNS sources in physiological and pathological conditions. Oxid Med Cell Longev 2016:1245049. https://doi.org/10.1155/2016/1245049
61. Boldrini M, Santiago AN, Hen R, Dwork AJ, Rosoklija GB, Tamir H, Arango V, John Mann J (2013) Hippocampal granule neuron number and dentate gyrus volume in antidepressant-treated and untreated major depression. Neuropsychopharmacology 38(6):1068–1077. https://doi.org/10.1038/npp.2013.5
62. Aleksandrova LR, Wang YT, Phillips AG (2019) Evaluation of the Wistar-Kyoto rat model of depression and the role of synaptic plasticity in depression and antidepressant response. Neurosci Biobehav Rev 105:1–23. https://doi.org/10.1016/j.neubiorev.2019.07.007